Resolving Halogen vs Hydrogen Bonding Dichotomy in Solutions: Intermolecular Complexes of Trihalomethanes with Halide and Pseudohalide Anions

Journal:	*Physical Chemistry Chemical Physics*
Manuscript ID	CP-ART-06-2018-003505.R2
Article Type:	Paper
Date Submitted by the Author:	06-Aug-2018
Complete List of Authors:	Watson, Brandon; Ball State University, Chemistry Grounds, Olivia; Ball State University, Chemistry Borley, William; Ball State University, Chemistry Rosokha, Sergiy; Ball State University, Chemistry

Resolving Halogen vs Hydrogen Bonding Dichotomy in Solutions: Intermolecular Complexes of Trihalomethanes with Halide and Pseudohalide Anions

Brandon Watson, Olivia Grounds, William Borley, Sergiy V. Rosokha[*]

Department of Chemistry, Ball State University, Muncie, IN, USA, 47306

Abstract

Halogen- and hydrogen-bonded complexes between trihalomethanes, CHX_3, and (pseudo-)halide anions, A^-, co-existing in acetonitrile solutions were identified and characterized via a combination of UV-Vis and NMR spectral measurements with the results of X-ray structural and computational analyses. Halogen-bonded [CHX_3, A^-] complexes displayed strong absorption bands in the UV range (showing Mulliken correlations with the frontier orbital energies of the interacting species) and the decreased shift of the NMR signal of trihalomethanes' protons. Hydrogen bonding led to the opposite (increased) NMR signal shift and the UV-Vis absorption bands of the hydrogen-bonded [CHX_3, A^-] complexes were similar in intensity to that of the separate CHX_3 molecules. The simultaneous multivariable treatment of the results of UV-Vis and NMR titrations of CHX_3 with A^- anions afforded formation constants of both halogen- and hydrogen-bonded complexes between these species, which existed side-by-side in the acetonitrile solutions. The relative values of the formation constants were consistent with the magnitudes of the positive potentials on the surfaces of the halogen or hydrogen atoms if the effects of the polarization of the trihalomethanes due to the presence of the anions were taken into account.

[*] Corresponding author, e-mail: svrosokha@bsu.edu, phone: + 1-765-285-8615.

Introduction

Halogenated molecules represent one of the most common types of electrophiles and their complexes with nucleophiles were described in chemical literature dating back more than a century.[1-4] A number of such complexes were characterized in solutions and in the solid state during the 1950s-1980s.[5-8] Following Mulliken, they were usually considered as a subclass of electron donor-acceptor (charge-transfer) complexes.[5-12] Yet, it was not until the early 2000s that the significance and ubiquity of halogen bonding was widely recognized by the scientific community. The current growth in interest in this supramolecular interaction was initiated largely by the works of Resnati, Metrangolo and co-workers who demonstrated its considerable potential for crystal engineering and molecular recognition.[13,14] The recent publications generally draw a parallel between halogen and hydrogen bonding (XB and HB, respectively).[15-17] These interactions are characterized by the comparable interaction energies and geometries.[3,4] They are also commonly related to the electrostatic attraction of the electron-rich centers to the area of positive potential on the surface of the (covalently-bonded) halogen or hydrogen atoms,[18,19] though the contributions of other components (e.g. charge-transfer) are also recognized.[3,20-24]

Since many molecules can participate in both XB and HB, accurate interpretations of intermolecular interactions in chemical and biochemical systems require identification and characterization of the co-existing modes of bonding. However, the relative strengths of these bonds were evaluated mainly *in silico*. The experimental data about the competition and cooperation of XB and HB interactions were obtained mostly via X-ray structural studies of the solid-state associates,[25-31]** where the presence or preference of a certain mode of intermolecular bonding is affected by the crystal packing forces. The solution-phase studies allow direct measurements of XB and HB thermodynamics and they provide important insight into the nature of these interactions. For example, Robertson et al. suggested the importance of the charge-transfer component in halogen bonding based on the solvent-resistance of XB of diiodine, as opposed to decreasing stability of HB-complexes of phenol derivatives with solvent polarity.[32] The earlier solution-phase measurements also revealed that HB and XB interactions led to opposite shifts of the proton NMR signals.[11] Based on the correlations between proton NMR shifts of haloforms and methylene halides in various solvents, Bertran and Rodriguez detected XB of these molecules with aza-aromatic solvents,[33] and estimated ranges of contributions of XB of

haloforms with different solvents' groups.[12]# Besides, earlier studies indicated that formation of XB complexes is accompanied by the appearance of absorption bands in the UV-Vis range, while HB usually leads only to the shift of the absorption bands of interacting species.[5,6,34-46] However, most of the previous studies compared XB and HB bonding involving related but different hydrogen or halogen-substituted molecules and measured separately.[33-35] The experimental identification of both types of complexes (and their equilibria constants) of the same molecule co-existing in solutions are lacking and the studies of such solution-phase competition of XB and HB interactions are scarce.[12,38,39] A latest excellent publication of Schulz et al.[39] represents a rare example of such work. In this comprehensive study, the relative strengths of the XB/HB interactions of haloimidazolium derivatives were measured experimentally, and the quantitative comparison of the interaction energies and free energies of different modes of association were derived from the quantum mechanics / molecular mechanics and classical molecular dynamics simulations.[39]

To explore XB/HB competition of the same molecule, we turned to the interaction of trihalomethanes, CHX_3 (X = I, Br, Cl) with (pseudo-)halide anions, A^- ($A^- = Cl^-$, Br^-, I^-, NCS^-, NCO^-, N_3^-). The CHX_3 molecules are among the simplest species capable of both interactions, and X-ray structural analysis revealed that their co-crystals with halides comprise both XB and HB modes of bonding (co-crystals of iodoform comprise mostly XB associates, and the majority of chloroform-containing structures show only hydrogen bonds).[47]& Based on the opposite directions of the proton NMR signal shift, Green and Martin suggested about 50 years ago that CHI_3 forms "*halogen bonds",* while $CHCl_3$ and $CHBr_3$ form preferably "*hydrogen bonds"* with halides in solutions.[11] In comparison, the earlier UV-Vis measurements indicated the formation of the halogen bonds between $CHBr_3$ and (pseudo-)halide anions.[49-51] Yet, the data treatments in these earlier studies were done assuming the presence of only one mode of bonding which might have led to substantial errors. In the current work, we combine UV-Vis and NMR studies with the computational analysis of the XB/HB complexes and their components. Such a comprehensive evaluation verifies *quantitatively* the dominance and/or coexistence of different modes of interaction of trihalomethanes. It also allows us to establish factors that determine bonding preferences of these prototypical HB/XB donors, as well as to clarify similarity and distinctions in the nature and characteristics of the XB and HB complexes.

Results and Discussion.

1. Spectral (UV-Vis and ^{1}H NMR) measurements of the complex formation of trihalomethanes with halide and pseudohalide anions.

A solution of CHI_3 in acetonitrile is characterized by absorption bands with maxima at 336 nm, 296 nm and 265 nm (Figure 1). Pseudohalide and halide anions do not absorb substantially in this spectral range. An incremental addition of any of these nucleophiles (taken as salts with Pr_4N^+ or Bu_4N^+ counter-ions) to the solution of CHI_3 results in the increase of intensity of the absorption in this area and gradual appearance of new absorption maxima (Figure 1 and Figures S1 - S6 in the ESI). The intensities of these new bands increase reversibly with the decrease of the temperature and Job's plots show a maximum at 1:1 molar ratios of components (Figure S7 in the ESI). All these data indicate that these bands are related to the formation of 1:1 complexes between triiodomethane and (pseudo-)halide anions:

$$CHI_3 + A^- \rightleftharpoons [CHI_3, A^-] \qquad (1)$$

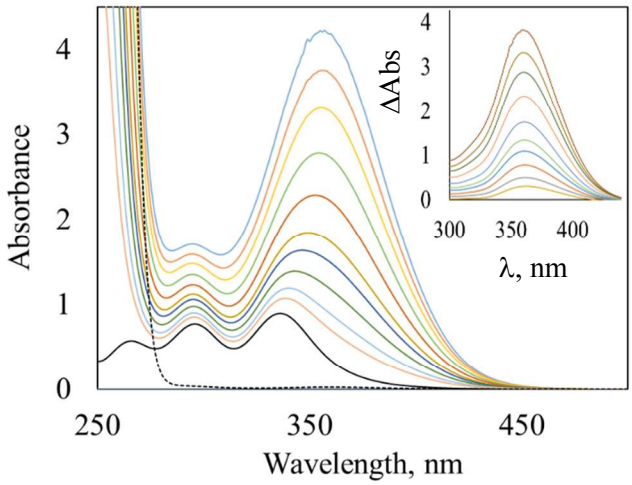

Figure 1. Spectra of acetonitrile solutions with constant concentration of CHI_3 (4.6 mM) and various concentrations of Pr_4NI (0, 4.6, 7.4, 12.4, 18.6, 24.8, 37.2, 54.6, 76.5, 98.3 and 131 mM, solid lines from the bottom to the top). Dashed line shows spectrum of the separate 200 mM solution of Pr_4NI. Insert: Spectra of the $[CHI_3, I^-]$ complex obtained by subtraction of the absorption of components from the spectra of their mixtures.

Absorption bands maxima and extinction coefficients are listed in Table 1. The energies of these bands show Mulliken correlations with the energies of the HOMOs of the anions suggesting their charge-transfer character (Figure S8 in the ESI).

Table 1. Spectral characteristics of [CHX_3, A^-] complexes in acetonitrile.

	CHI_3		$CHBr_3$		$CHCl_3$[b]
A^-[a]	λ_{max}, nm (ε, 10^3 $M^{-1}cm^{-1}$)[c]	$\Delta\delta_\infty$, ppm[d]	λ_{max}, nm (ε, 10^3 $M^{-1}cm^{-1}$)[c]	$\Delta\delta_\infty$, ppm[d]	$\Delta\delta_\infty$, ppm[d]
I^-	314sh 357(11.5)	-0.23	294[e]	0.97	1.80
Br^-	297 (9.5) 335sh	-0.23	259 (9.8)[f]	1.34	2.05
Cl^-	279(4.0) 333(1.8)	-0.27	<230[e]	1.54	2.49
NCS^-	310(9.0) 346sh	-0.15	275[g]	0.80	1.04
NCO^-	278 (6.2) 322(2.7)	-0.20	245[g]	-	-
N_3^-	320 sh 355(8.0)	-0.20	294[g]	-	-

a) Taken as Bu_4NA or Pr_4NA salts. b) Absorption bands of the complexes were overshadowed by the absorption of components and solvent. c) From the fitting assuming formation of only XB complex). d) Limiting shift of the proton NMR signal, from the fitting assuming formation of only HB complex. e) Ref. [51]. f) Ref. [49]. g) Ref. [50].

In accordance with the earlier data,[11] NMR measurements showed that the addition of the (pseudo-)halide anions to solutions of iodoform in CD_3CN resulted in the decreased shift of the proton signal of CHI_3 (Figure 2 and Figure S9 in the ESI). This suggests a dominance of XB in these solutions. The dependence of the NMR shifts (Δδ) on the concentration of anions can be fitted using a model that takes into

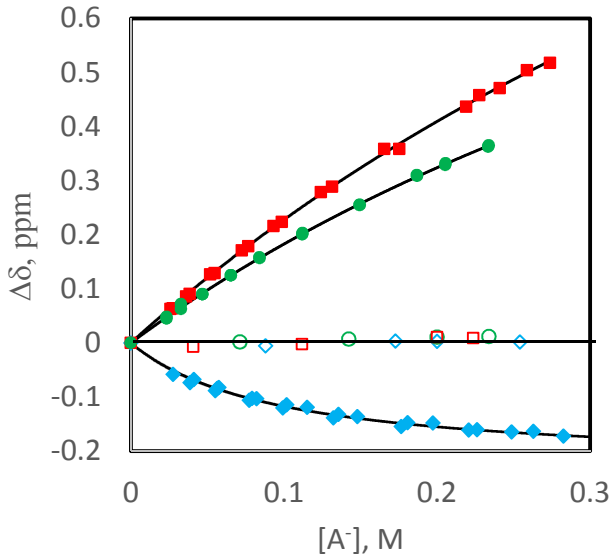

Figure 2. Dependencies of proton NMR shifts of CHX_3 (in CD_3CN, 22°C, relative to that in the separate molecules) on the concentration of added Pr_4NA salts. Filled symbols show proton shifts of CHI_3 (♦), $CHBr_3$ (●), $CHCl_3$ (■) in the presence of bromide ($A^- = Br^-$) and open symbols show essential independence of shifts of CHI_3 (◊), $CHBr_3$ (○) and $CHCl_3$ (□) on concentrations of (non-bonding) BF_4^- anions ($A^- = BF_4^-$). Concentrations of CHI_3 (5.2 mM), $CHBr_3$ (5.0 mM), and $CHCl_3$ (5.0 mM) were constant during titrations.

account formation of only one complex. Such fitting produced formation constants of the complexes (K_{NMR}^{eff} in Table S1 in the ESI), as well as the values of the limiting shift, $\Delta\delta_\infty$ (Table 1). Analogous treatment of the UV-Vis data (Figures S1C – S6C in the ESI) afforded formation constants $K_{UV}^{eff,}$ which were generally consistent with the corresponding values of K_{NMR}^{eff} (Table S1 in the ESI). It confirmed that the new absorption bands are related to the formation of the XB complexes.

UV-Vis spectra of the mixtures of $CHCl_3$ with the (pseudo-)halide anions in acetonitrile did not show new bands at $\lambda > 200$ nm. NMR measurements revealed that the addition of these anions to the solutions of chloroform in acetonitrile led to an increase of its proton shift (Figure 2 and Figure S12 in the ESI).

Addition of the (pseudo-)halide anions to the solution of $CHBr_3$ led to the appearance of new absorption bands in the UV range indicating formation of the 1:1 [$CHBr_3$, A^-] complexes (Figure S10 in the ESI).[49-51] The absorption band maxima of these complexes were blue-shifted as compared to that of iodoform and their energies followed analogous Mulliken correlation (Figure S8 in the ESI) suggesting their common (XB) nature.§ Yet, NMR measurements showed that the addition of these anions to bromoform resulted in an increased shift of the signal of the $CHBr_3$ proton (Figure 2 and Figure S11 in the ESI). This indicated the formation of HB complexes between $CHBr_3$ and the (pseudo-)halide anions.[11] Since the spectral changes measured by NMR and UV-Vis were determined by two different processes (HB and XB, respectively), the values of the effective constants K_{UV}^{eff} and K_{NMR}^{eff} obtained by treatments of these data assuming formation of only one type of complex were quite different (Table S1 in the ESI). Evidently, the assumption that only one type of complex is formed in these systems is incorrect. Also, while XB is a dominant mode of interaction of iodoform with anions, the HB complexes may be also present in their solutions and distort calculations of the formation constants.

The accurate treatment of the equilibria in CHX_3/X^- solutions should take into account formation of XB and HB associates, and the resulting formation constants of these complexes should describe consistently UV-Vis and NMR changes. To verify characteristics of the XB and HB complexes, necessary for such evaluations of both constants, we carried out their computational analyses, as follows.

2. Computational characterization of the intermolecular associates of trihalomethanes

The geometries of $CHX_3 \cdot A^-$ complexes were fully optimized via DFT (M062X/def2tzvpp) computations in the gas phase and in acetonitrile (see the ESI for the details, note that since UV-Vis and NMR measurements were carried out in CH_3CN, the following discussion will focus on the data calculated in this medium). For all $CHX_3 \cdot A^-$ pairs, these computations afforded energy minima corresponding to XB and HB interactions (Figure S20 in the ESI).[¶] The calculated energies and geometric characteristics of all complexes are listed in the Tables S3 and S4 in the ESI. The variations of the interaction energies, ΔE, in acetonitrile with the nature of the CHX_3 and anions are shown in Figure 3.

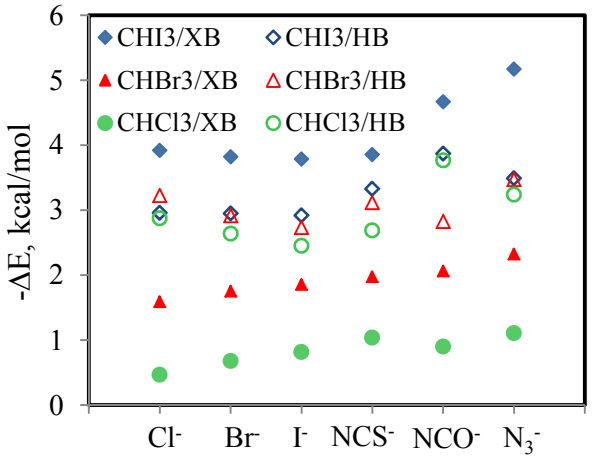

Figure 3. Interaction energies in the XB and HB complexes of CHX_3 with A^- anions (as indicated, in CH_3CN).

The HB complexes show minor dependence of ΔE on the nature of CHX_3 and anions (ΔE = -3.0 ± 0.5 kcal/mol). In comparison, the ΔE values of the XB complexes vary significantly with CHX_3. The complexes of $CHBr_3$ are less stable (by 2 - 3 kcal/mol) than the corresponding associates of CHI_3, and $CHCl_3$ forms the weakest XB complexes. Thus, in accordance with the experimental data, the XB complexes of CHI_3 are more stable than the corresponding HB associates, while the $CHBr_3$ and $CHCl_3$ electrophiles show the opposite relationship between the stability of their XB and HB complexes. The ΔE values calculated in the gas phase are higher and they showed similar trends (Table S3B in the ESI).

The intermolecular separations in the complexes calculated in acetonitrile (Tables S4 in the ESI) are consistent with the X-ray structural data. For example, the calculated X…A^- distances in the XB complexes of iodoform are 3.111 Å, 3.312 Å and 3.569 Å for dyads with A^- = Cl^-, Br and I^-, respectively. In comparison, the average X…A^- separations in the co-crystals of CHI_3 with tetraalkylammonium salts of Cl^-, Br^- and I^- anions are 3.130 Å, 3.254 Å and 3.551 Å, respectively (Table S7 in the ESI). The C-X…A^- angles in all calculated and solid-state associates were close to 180°. The normalized separations R_{XA} (R_{XA}= $d_{XA}/(R_X + R_A)$, where d_{XA} are H…A or X…A separation, and R_X and R_A are van der Waals radii) for the HB complexes of different CHX_3 molecules with the same nucleophile are very close (see Figure S21 in the ESI). The XB complexes show more substantial dependence of R_{XA} values on the nature of the CHX_3. With each anion, they are increasing in the order $CHI_3 < CHBr_3 < CHCl_3$. Among different halides, the R_{XY} values are increasing in the order Cl^- (0.83) < Br^- (0.87) < I^- (0.90), in accordance with the values of 0.84 (Cl^-), 0.86 (Br^-) and 0.90 (I^-) measured in the solid-state associates.

The TD-DFT computations produced absorption bands in the UV spectra of all [CHX_3, A^-] complexes (Table S5 in the ESI). The intensities of the absorption bands of the HB complexes (log ε_{HB} ~ 10^3 M^{-1} cm^{-1}) are close to that of the separate CHX_3 molecules (Figure S22 and Table S5 in the ESI). The intensities of the calculated absorption bands in the XB complexes, ε_{XB}, are about an order of magnitude higher than those of the separate trihalomethanes. Also, the variations of the calculated log ε_{XB} values are consistent with the experimental UV-Vis data. The average difference between the corresponding calculated and experimental values, $\Delta = 1/n \times (\Sigma (\log \varepsilon_{XB} - \log \varepsilon_{exp})$, is 0.01 (Table S5 in the ESI). This confirms that the increase of the intensity of the absorption in the solution of CHX_3 upon addition of anions is related to the formation of XB complexes.[†]

The GIAO calculations showed that the XB results in the shielding of the CHX_3 proton as compared to the isolated molecules (i.e. $\Delta\delta_{XB}$ are negative). The proton signals in the HB complexes are deshielded and the magnitudes of the shift, $\Delta\delta_{HB}$, were larger than those resulting from halogen bonding, $\Delta\delta_{XB}$ (Table 2).

Table 2. Calculated NMR proton shifts, $\Delta\delta_{XB}$ and $\Delta\delta_{HB}$ of CHX_3 molecules in the XB and HB complexes (relative to that for the separate molecules).[a]

A^-	CHI_3		$CHBr_3$		$CHCl_3$	
	$\Delta\delta_{XB}$	$\Delta\delta_{HB}$	$\Delta\delta_{XB}$	$\Delta\delta_{HB}$	$\Delta\delta_{XB}$	$\Delta\delta_{HB}$
Cl^-	-0.61	2.91	-0.35	3.14	-0.34	2.99
Br^-	-0.54	2.25	-0.31	2.58	-0.32	2.24
I^-	-0.49	1.42	-0.28	1.87	-0.31	1.51
N_3^-	-0.64	2.33	-0.26	2.83	-0.25	2.28
NCS^-	-0.45	0.98	-0.22	0.99	-0.24	0.87
NCO^-	-0.53	2.82	-0.28	3.13	-0.25	2.67
	$(\Delta\delta_\infty/\Delta\delta_{XB})^b = 0.40 \pm 0.07$		$(\Delta\delta_\infty/\Delta\delta_{HB})^b = 0.58 \pm 0.15$		$(\Delta\delta_\infty/\Delta\delta_{HB})^b = 1.04 \pm 0.19$	

a) In ppm, in CD_3CN. $\Delta\delta_{XB} = \delta_{XB} - \delta_o$ and $\Delta\delta_{HB} = \delta_{HB} - \delta_o$ where δ_{XB}, δ_{HB} and δ_o are calculated shifts in the XB, HB complexes and in the separate molecules, respectively). b) Average ratios (and their standard deviations) of experimental $\Delta\delta_\infty$ values (Table 1) to the calculated values for the dominant for this CHX_3 molecule interaction.

Comparison with the experimental data in Table 1 revealed that the calculated values of $\Delta\delta_{HB}$ for the complexes of chloroform were within 20% of the $\Delta\delta_\infty$ values. It suggested that the calculations reproduced $\Delta\delta_{HB}$ values reasonably well and that XB has negligible effects on the NMR measurements of complex formation between $CHCl_3$ and A^- anions. The $\Delta\delta_\infty$ values resulting from the measurements with $CHBr_3$ (Table 1) were significantly lower than the calculated $\Delta\delta_{HB}$ values. The average value of $\Delta\delta_\infty/\Delta\delta_{HB}$ of about 0.6 in these systems implies the presence of significant amounts of XB complexes (which shifts a proton signal in the opposite direction). Since XB was a dominant mode of interaction in the solutions of iodoform, the $\Delta\delta_\infty$ values for these pairs were compared with the calculated $\Delta\delta_{XB}$ values. The $\Delta\delta_\infty/\Delta\delta_{XB}$ ratio for these systems is about 0.4. Since the magnitudes of $\Delta\delta_{HB}$ are larger than those of $\Delta\delta_{XB}$, the presence of smaller fractions of the HB complexes has more significant effects on the chemical shifts in the mixtures of CHI_3 with anions than the comparable fractions of XB complexes in the solutions of $CHBr_3$.

Overall, the calculated characteristics of the XB and HB complexes were consistent with the experimental data. They showed that XB is a dominant mode of interaction of CHI_3 with A^-, and that the XB complexes [CHI_3, A^-] are characterized by the strong UV-Vis absorption bands in the 250 - 400 nm range and by decreased shifts of the proton NMR signal. However, the small $\Delta\delta_\infty/\Delta\delta_{XB}$ values suggested

the presence of the HB complexes in the solutions with iodoform, which were neglected in the previous treatments. In contrast, HB is a dominant mode of interaction of chloroform. This bonding leads to the increased shift of the proton NMR signal and does not produce new intense absorption bands in the UV-Vis range. The XB complexes of $CHCl_3$ are much weaker than their HB associates and they show absorption bands around 200 nm. As such, even if small amounts of XB complexes are present in the solutions containing $CHCl_3$ and anions, they have negligible effects on the NMR spectra and their UV-Vis bands are overshadowed by the absorption of the reactants. Bromoform represents an intermediate case. The calculated HB complexes of $CHBr_3$ are more stable than the XB associates (Figure 3). However, the differences of the ΔE values are rather small, in accordance with UV-Vis and NMR measurements, which showed the presence of both XB and HB complexes in the solutions of $CHBr_3$ with A^- anions.

3. Formation constants of the coexisting XB and HB complexes.

In general, the addition of A^- anions to the solutions of CHX_3 molecules leads to the formation of XB and HB complexes with the equilibrium constants K_{XB} and K_{HB}, respectively (eqs 2 and 3):

$$CHX_3 + A^- \overset{K_{XB}}{\rightleftharpoons} [X_2HC\text{-}X\cdots A^-] \quad (2)$$

$$CHX_3 + A^- \overset{K_{HB}}{\rightleftharpoons} [X_3C\text{-}H\cdots A^-] \quad (3)$$

The analysis of the experimental and computational data point out that the formation of the triple complexes can be neglected under experimental conditions (see the ESI for details). Therefore:

$$K_{XB} = C_{XB} / ((C^o_D - C_{XB} - C_{HB})(C^o_A - C_{XB} - C_{HB})) \quad (4)$$

$$K_{HB} = C_{HB} / ((C^o_D - C_{XB} - C_{HB})(C^o_A - C_{XB} - C_{HB})) \quad (5)$$

where C_{XB} and C_{HB} are equilibrium concentrations of XB and HB complexes, and C^o_D and C^o_A are initial concentrations of CHX_3 and A^-, respectively. Solving this system of two equations gives C_{XB} and C_{HB} as:

$$C_{XB} = \{(C^o_A + C^o_D + 1/(K_{XB}+K_{HB})) - ((C^o_A + C^o_D + 1/(K_{XB}+K_{HB}))^2 - 4C^o_A C^o_D)^{0.5}\}/(2(1+K_{HB}/K_{XB})) \quad (6)$$

$$C_{HB} = \{(C^o_A + C^o_D + 1/(K_{XB}+K_{HB})) - ((C^o_A + C^o_D + 1/(K_{XB}+K_{HB}))^2 - 4C^o_A C^o_D)^{0.5}\}/(2(1+K_{XB}/K_{HB})) \quad (7)$$

Since the UV-Vis spectral changes are mainly related to the formation of XB complexes,[$]

$$\Delta Abs = \varepsilon l \times C_{XB} \quad (8)$$

where ε is an extinction coefficient of the XB complex and l is a length of a cuvette. The NMR shifts, $\Delta\delta$ is determined by the (opposite) contributions of the XB and HB complexes, $\Delta\delta_{XB}$ and $\Delta\delta_{HB}$:

$$\Delta\delta = \Delta\delta_{XB}C_{XB}/C^{o}_{D} + \Delta\delta_{HB}C_{HB}/C^{o}_{D} \quad (9)$$

Substituting C_{XB} and C_{HB} in eqs 8 and 9 using eqs 6 and 7 presents ΔAbs and Δδ as functions of the known C^{o}_{D} and C^{o}_{A} values, as well as unknown values of K_{XB}, K_{HB}, ε, $\Delta\delta_{XB}$, and $\Delta\delta_{HB}$.

$$\Delta Abs = \varepsilon l \times \{(C^{o}_{A}+C^{o}_{D}+1/(K_{XB}+K_{HB}))-((C^{o}_{A}+C^{o}_{D}+1/(K_{XB}+K_{HB}))^{2} - 4C^{o}_{A}C^{o}_{D})^{0.5}\}/(2(1+K_{HB}/K_{XB})) \quad (10)$$

$$\Delta\delta = \Delta\delta_{XB}/C^{o}_{D}\times\{(C^{o}_{A}+C^{o}_{D}+1/(K_{XB}+K_{HB}))-((C^{o}_{A}+C^{o}_{D}+1/(K_{XB}+K_{HB}))^{2}-4C^{o}_{A}C^{o}_{D})^{0.5}\}/(2(1+K_{HB}/K_{XB})) +$$
$$+ \Delta\delta_{HB}/C^{o}_{D}\times\{(C^{o}_{A}+C^{o}_{D}+1/(K_{XB}+K_{HB}))-((C^{o}_{A}+C^{o}_{D}+1/(K_{XB}+K_{HB}))^{2}-4C^{o}_{A}C^{o}_{D})^{0.5}\}/(2(1+K_{XB}/K_{HB})) \quad (11)$$

Simultaneous fittings of the dependences of two variables, ΔAbs and Δδ, on C^{o}_{A} (at constant C^{o}_{D}) may, in principle, afford the values of all five unknowns. Yet, the 5-parameters fitting produced unreliable results with the errors exceeding 100% (see the ESI for details). As such, the UV and NMR data were fitted using three variable parameters (K_{HB}, K_{XB} and ε), while the fixed $\Delta\delta_{XB}$ and $\Delta\delta_{HB}$ values were taken from the computations (Table 2). The simultaneous multivariable fittings of the dependences of ΔAbs and Δδ values on the concentration of I^- anions in the solutions with the constant concentrations of either CHI_3 or $CHBr_3$ are illustrated in Figure 4. The fittings of the UV-Vis and NMR data for all donor/acceptor pairs (together with the corresponding statistical data) are shown in Figures S13 - S19 in the ESI. Such

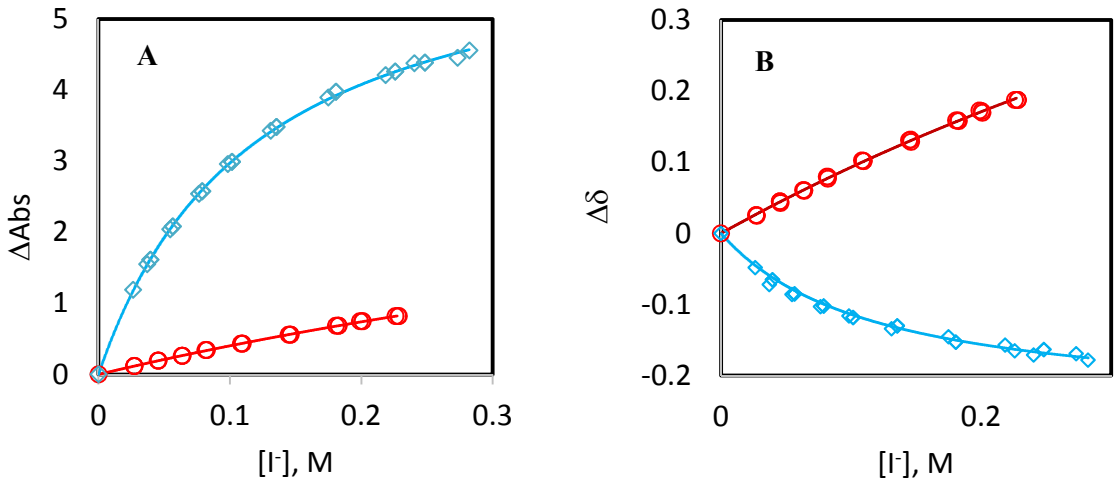

Figure 4. Dependencies of the (A) and Δδ (B) values in the solutions of $CHBr_3$ (○) and CHI_3 (◊) on concentration of iodide. Solid lines show calculated values resulted from the simultaneous multivariable fitting of the UV-Vis and NMR titrations data. (Note that ΔAbs were measured at λ = 290 nm and 357 nm for $CHBr_3$ and CHI_3, respectively, concentrations of $CHBr_3$ and CHI_3 were 5.0 mM and 5.2 mM, respectively, and iodide was taken as Bu_4N salt).

fittings produced the values of the formation constants of the competing HB and XB complexes, K_{HB} and K_{XB}. These values are listed in Table 3 (the standard deviations were ~ 1 - 3% and R^2 values were higher than 0.998, see statistical data in Figures S13 – S19 in the ESI).

Table 3. Formation constants K_{XB} and K_{HB} of the co-existing XB and HB complexes of iodoform or bromoform resulted from the simultaneous multivariable fitting of the UV-Vis and NMR data.[a]

	$CHBr_3$		CHI_3	
A^{-b}	K_{XB}, M^{-1}	K_{HB}, M^{-1}	K_{XB}, M^{-1}	K_{HB}, M^{-1}
I^-	0.39	0.60	7.7	1.1
Br^-	0.52	0.87	9.4	1.2
Cl^-	-	-	11.0	1.4
NCS^-	0.09	0.43	1.7	0.4
N_3^-	0.27	0.59	7.6	1.2

a) In acetonitrile (CH_3CN or CD_3CN), at 22°C. b) Taken as Pr_4NA or Bu_4NA salts.

Using the model that takes into account formation of both XB and HB complexes, the spectral data can be treated separately, i.e. UV-Vis and NMR data can be fitted to eqs 10 and 11, respectively. The separate fittings of the NMR data using eq 11 (with two variable parameters, K_{HB} and K_{XB} and fixed $\Delta\delta_{XB}$ and $\Delta\delta_{HB}$ values) yielded formation constants K_{HB} and K_{XB} which are consistent with the values obtained from the simultaneous fittings (Table S2 in the ESI). However, the errors resulting from such separate fittings are about three times larger than that of the combine fittings. The separate three-parameters ($K_{HB,}$ K_{XB} and ε) fittings of ΔAbs (eq 10) yielded even large standard errors (Table S2 in the ESI). However, since the fitting of $\Delta\delta$ depends on the calculated $\Delta\delta_{XB}$ and $\Delta\delta_{HB}$, the simultaneous fitting of the UV-Vis data (which do not depend on these parameters) using the same K_{HB} and K_{XB} values verifies the formation constants. Overall, the data in Table S2 in the ESI confirm that the simultaneous treatments of the UV-Vis and NMR data provide more accurate and reliable data than their separate fittings.

It should be also stressed that in addition to the UV-Vis and NMR data, our evaluation of thermo-dynamics of the competing XB and HB interactions is based on the values of $\Delta\delta_{XB}$ and $\Delta\delta_{HB}$ obtained from the computational analysis of the corresponding complexes. As described in section 2, the validity of the latter is supported by the good correlation of the characteristics of calculated complexes with the

experimental data. Besides, the same values of the equilibria constants allowed to fit both NMR and UV-Vis data (vide supra) and their relative values are consistent with the surface electrostatic potentials, as follows.

4. **Variations of the equilibria constants vs surface electrostatic potentials.**

The data in Table 3 demonstrate that XB and HB complexes of $CHBr_3$ are characterized by comparable formation constants, although HB is somewhat stronger. XB is a predominant mode of interaction of CHI_3, but formation constants of its HB complexes are also substantial. In fact, the K_{HB} values for the complexes of iodoform are mostly higher than the K_{XB} and K_{HB} values for the complexes of bromoform. To check the reasons of such variations, we carried out calculations of the electrostatic surface potentials (ESP) of the CHX_3 molecules. These calculations revealed the areas of the positive potentials on the surfaces of their halogen and hydrogen substituents along the C-H and C-X bonds (Figure 5). The values of the maximum potentials on the surfaces of these atoms, V_{max}^{X} and V_{max}^{H}, are listed in Table 4.

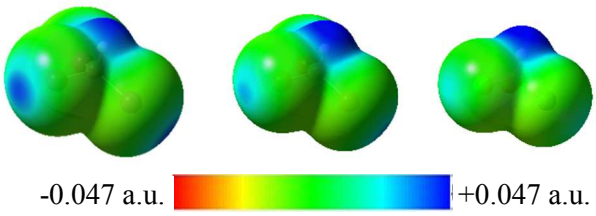

Figure 5. Electrostatic potential on the molecular surfaces of CHI_3 (left), CHBr3 (center) and $CHCl_3$ (right) electrophiles (from M062X/def2tzvpp calculations at 0.001 a.u. electronic density).

Table 4. Maximum positive potentials (in a.u.) on the surfaces of halogen (V_{max}^{X}) and hydrogen (V_{max}^{H}) atoms in the isolated CHX_3 molecules and in the molecules polarized by the negative charge.

	$CHCl_3$	$CHBr_3$	CHI_3
V_{max}^{X} [a]	0.0200	0.0302	0.0425
V_{max}^{H} [a]	0.0624	0.0611	0.0541
V_{max}^{X}(XB) [b]	0.0280	0.0771	0.1281
V_{max}^{H}(HB) [c]	0.0685	0.0893	0.0917

a) Isolated molecule. b) Calculated in a presence of a negative charge located at the position of Br^- anion in the XB [CHX_3, Br^-] complexes. c) Calculated in a presence of a negative charge located at the position of Br^- anion in the HB [CHX_3, Br^-] complexes.

The V_{max}^{X} values in CHX_3 molecules increase substantially in the order Cl < Br < I. The V_{max}^{H} values are changing in the opposite direction, but their variations are less pronounced than that of V_{max}^{X}. Most notably, while $V_{max}^{H} > V_{max}^{X}$ for all isolated CHX_3 molecules, halogen bonding is the dominant mode of interaction of iodoform. To explain this apparent discrepancy, we looked at the V_{max}^{X} and V_{max}^{H} values in the presence of the anions (since the surface potentials of trihalomethanes could be significantly altered due to polarization[18,19]). Specifically, we performed ESP computations in the presence of the (-1) charge placed at the positions occupied by the Br^- anions in their optimized HB and XB complexes. The values of the maximum potentials on the surfaces of the interacting (X or H) atoms in the molecules polarized by the halogen-bonded and hydrogen-bonded bromides are designated in Table 4 as $V_{max}^{X}(XB)$ and $V_{max}^{H}(HB)$, respectively. The data in Table 4 indicate that $V_{max}^{X}(XB) > V_{max}^{X}$ for all molecules and the increase of the potential on the surface of the halogen atom due to polarization is most pronounced in the case of iodoform. The increase of V_{max}^{H} due to polarization of CHX_3 molecules by hydrogen-bonded bromide is smaller. As a result, the maximum potential on the surface of iodine in the XB-polarized iodoform is higher than that on the surface of hydrogen in the HB-polarized CHI_3 (i.e. $V_{max}^{X}(XB) > V_{max}^{H}(HB)$). In contrast to iodoform, the maximum potentials on the surfaces of hydrogen atoms in polarized bromoform and chloroform are higher than that on the surfaces of the halogen atoms (although, for bromoform, the difference is less pronounced than that in the isolated molecule). As such, the relative values of maximum potentials of the polarized molecules are consistent with the predominance of XB or HB mode in the solutions of trihalomethanes. Moreover, comparison of the data in Tables 3 and 4 revealed a close correlation between the formation constants of the XB and HB complexes of iodoform and bromoform measured with a certain anion and the maximum potential values on the surfaces of the (X or H) atoms involved in intermolecular bonding, $V_{max}^{X}(XB)$ or $V_{max}^{H}(HB)$. In fact, the values of four constants measured with each anion (two with $CHBr_3$ and two with CHI_3) are proportional to the magnitude of the σ-hole on the atom to which this anion is bonded (i.e. they fall on the same trend line) regardless of the mode of interaction (Figure 6).

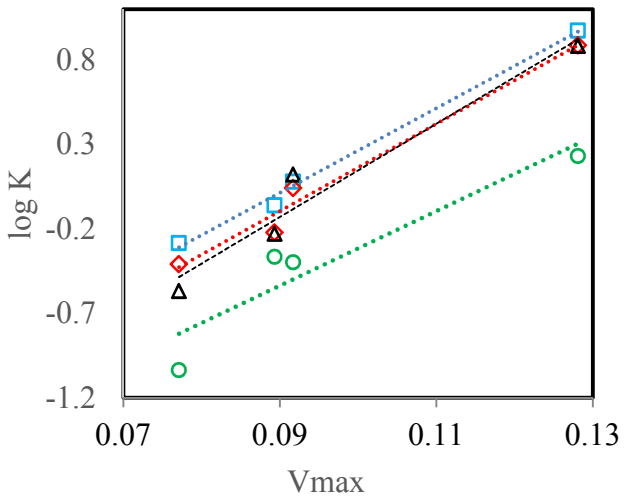

Figure 6. Correlations between the formation constants of XB and HB complexes [CHX_3, A^-] and V_{max} values (either V_{max}^X(XB) or V_{max}^H(HB)) on the surfaces of the halogen or hydrogen atoms in the appropriately polarized CHI_3 and $CHBr_3$ molecules. A^- = Br^-(□), I^-(◊), NCS^-(○) and N_3^- (Δ).

The correlation between log K and V_{max} values for the complexes with Br^- anions is characterized by the highest R^2 of 0.995. This is apparently related to the fact that V_{max}^H(HB) and V_{max}^X(XB) were evaluated in the presence of the charges at the positions of the Br^- anions in their HB and XB complexes. Yet, the complexes with I^-, N_3^-, and NCS^- also show strong correlations of log K and V_{max} values (with R^2 of 0.98, 0.95 and 0.88, respectively), even though the effects of polarization in these complexes are expected to be somewhat different than that in [CHX_3, Br^-]. Such correlations indicate that the σ-hole model accounts for the variations of formation constants of these complexes (regardless of the mode of interaction), provided that the effects of the polarization of the latter are taken into account. On the other hand, these strong correlations support the validity of the K_{XB} and K_{HB} values resulting from the multivariable fitting.

Finally, it should also be mentioned that while the σ-hole model accounts for the variations of the formation constants values, it does not explain the drastic differences in their UV-Vis absorption spectra between the XB and HB complexes. The strong absorption bands of XB complexes suggest that this mode of interaction of CHX_3 molecules involves significant molecular-orbital interaction.[52]

Conclusions.

1. UV-Vis and NMR measurements and computational studies of the intermolecular interaction between trihalomethanes and (pseudo-)halide anions demonstrated that halogen bonding results in the appearance of strong absorption bands in the UV range and leads to the shielding (decrease of NMR shift) of the proton of trihalomethanes. In comparison, hydrogen-bonded complexes are characterized by a significantly increased shift of the proton NMR signals and by the absorption bands of about the same intensity as in the corresponding separate CHX_3 molecules.

2. Simultaneous treatments of the UV-Vis and NMR data confirmed the co-existence of both XB and HB complexes in acetonitrile solutions containing (pseudo-)halide anions and CHI_3 or $CHBr_3$ and allowed to evaluate (using the values of the NMR shifts from their computational studies) formation constants of the competing complexes formed by the same molecule. In general, such treatments can be used for resolving competing XB and HB interactions (or other modes of supramolecular bonding) based on the combination of different types of measurements. (In comparison, in the earlier work of Bertran and Rodriguez, the ranges of XB contributions in various groups of neat solvents, e.g. 0 - 15% for esters or 60 - 95 % for amines, were estimated using correlations between NMR signal shifts of $CHCl_3$ and CHI_3 or $CHCl_3$ and $CHBr_3$ measured in these solvents.[12]#) Our results also demonstrated that while the separate UV-Vis and NMR data can be seemingly fitted quite well assuming formation of only one type of supramolecular complex, the neglect of the second mode of interaction results in substantial errors in the equilibria constants of the dominant mode and the absence of values for the weaker mode (compare formation constants in Table 3 with that in Table S1 in the ESI).

3. Our work also demonstrated the significance of effects of polarizations in intermolecular bonding. Indeed, the earlier studies commonly considered correlations between strengths of intermolecular interactions and the V_{max} values evaluated in the unperturbed molecules (i.e. prior to interaction). Yet, this Level 1 (according to Clark[19]) approach led to the apparent contradiction between the relative formation constant values of XB and HB complexes of iodoform and the V_{max} values on surfaces of hydrogen and halogen substituents of the isolated CHI_3 molecule (i.e. $K_{XB} > K_{HB}$, but $V_{max}^{X} < V_{max}^{H}$). However, when

polarization of CHI_3 and $CHBr_3$ by anions in their XB and HB complexes was taken into account (Level 2 according to Clark[19]), the formation constants of these complexes showed strong correlations with the values of V_{max} on the surfaces of the atoms involved in the intermolecular bonding regardless of the mode of interaction and the nature of the interacting atom.

Experimental Section.

Commercially available trihalomethanes were purified by distillation or sublimation. UV-Vis and NMR measurements were carried out using tetrapropyl- and tetrabutylammonium salts of (pseudo-)halide anions which were prepared or purified as described earlier.[50,51] The UV-Vis spectra were measured on a Cary 5000 spectrophotometer in dry (HPLC grade) acetonitrile. NMR measurements were performed on a 400 MHz spectrometer in deuterated acetonitrile with an internal TMS standard. The intensities of the absorption of $[CHX_3, A^-]$ complexes, ΔAbs, were obtained by the subtraction of the absorption of the components from the spectrum of the CHX_3 and A^- mixtures. The ε values in Table 1 and K_{UV}^{eff} in Table S1 were obtained via the Benesi-Hildebrand procedure and by fitting the dependencies of ΔAbs on the concentrations of anions (assuming one 1:1 complex formation) using Origin Pro 2016. The values of $\Delta\delta_\infty$ (and K_{NMR}^{eff} in Table S1) were obtained by the similar treatment of the variations of the proton NMR signal shifts with the concentrations of anions. They represent the average values from the three-five series of UV-Vis and NMR measurements for each pair. The K_{XB} and K_{HB} values were obtained by the simultaneous nonlinear fitting (multiple variable option with Levenberg-Marquardt iteration algorithm in OriginPro 2016) of the dependencies of ΔAbs and $\Delta\delta$ on the concentrations of anions measured at the same concentrations of CHX_3 (eqs 10 and 11) with C^o_A as the independent variable, ΔAbs and $\Delta\delta$ as the dependent variables, K_{HB}, K_{XB} and ε as the adjustable parameters and with the constants $\Delta\delta_{XB}$ and $\Delta\delta_{HB}$ (from Table 2) and C^o_D. These fittings are illustrated in Figures S13 – S19. The details of all experiments and their treatments are described in the ESI.

Co-crystals of CHI_3 and with Pr_4NCl, Pr_4NBr or Bu_4NI for X-ray measurements were obtained by diffusion of hexane into dichloromethane solutions containing a 1:1 molar ratio of reactants at -20^o C.

Crystallographic, data collection and structure refinement details, as well as geometric characteristics of the halogen bonds in these crystals are presented in the ESI. Complete crystallographic data, in CIF format, have been deposited with the Cambridge Crystallographic Data Centre. CCDC 1837582, 1837583 and 1837584 contain the supplementary crystallographic data for this paper. These data can be obtained free of charge via www.ccdc.cam.ac.uk/data_request/cif.

The geometries of the XB and HB complexes and their components were optimized without constraints via DFT (M06-2X/def2tzvpp) calculations using the Gaussian 09 suite of programs.[53,54] Geometry optimizations in acetonitrile were carried out using the polarizable continuum model (PCM).[55] The interaction energies were determined as: $\Delta E = E_{comp} - (E_{CHX3} + E_A) + BSSE$, where E_{comp}, E_{CHX3} and E_A are sums of the electronic and zero-point energies of the complex, CHX_3 and anion and BSSE is a basis set superposition error. UV-Vis spectra of complexes and trihalomethanes were calculated via TD-DFT calculations, and proton NMR shifts were obtained via GIAO calculations using geometries of the complexes optimized in acetonitrile. Electrostatic potentials were calculated on 0.001 electrons $bohr^{-3}$ molecular surfaces. Details of the calculations, energies, geometric and spectral characteristics of HB and XB complexes, as well as atomic coordinates of the calculated complexes, are listed in the ESI.

Acknowledgements. We thank the National Science Foundation for the financial support of this work (grant CHE-1607746). We also thank Shubhangi Joshi for the initial UV-Vis measurements of the complexes between CHI_3 and A^- anions, Charlotte Stern for the X-ray measurements of the $Pr_4NCl \cdot CHI_3$ and $Pr_4NBr \cdot CHI_3$ co-crystals and Matthias Zeller for the X-ray measurements of the $Bu_4NI \cdot CHI_3$ co-crystal (the latter were supported by the National Science Foundation through the Major Research Instrumentation Program under Grant No. CHE 1625543: funding for the single crystal X-ray diffractometer).

References and Notes.

**Due to a large number of computational and X-ray crystallographic studies of co-existing HB and XB interactions, only a few representative examples[26-31] are cited herein.

[&]The Cambridge Crystallographic Database contains about a dozen X-ray structures comprising iodoform and halides. Most of them show XB between CHI_3 and anions,[56-60] although a few structures also comprise HB.[56,59] The majority of X-ray structures comprising $CHBr_3$ and halide anions show both HB and XB interactions,[36,61] and a crystal with only the HB mode is also available.[62] There are also about 270 structures containing $CHCl_3$ and halides with the intermolecular C-H…X^- distance of 0.1Å or more shorter than the sum of van der Waal radii and C-H-X angle between 150 and 180 deg, and about 70 chloroform-containing structures with similar C-Cl…X^- contacts.[47]

[#] Bertran and Rodrigues measured chemical shifts of CHX_3 (X = Cl, Br, I) in 24 solvents relative to that in cyclohexane and built correlations between values for $CHCl_3$ vs those for $CHBr_3$ or CHI_3. The XB fractions were estimated as $(\Delta_{HB}-\Delta_X)/\Delta_{HB}$, where Δ_X is experimental value of shift, Δ_{HB} is the HB shift taken as the value at the correlation line (the shifts of XB complexes were neglected).[12]

[§] The comparison with the spectra of the reported earlier complexes of (pseudo-)halides with the other bromine-containing electrophiles, e.g. CBr_4, CBr_3NO_2, CBr_3F,[50,51] showed that their absorption bands follow the same Mulliken correlation (Figure S8 in the ESI). Since the other electrophiles do not have hydrogen substituents, this common correlation suggests similar XB nature of all complexes.

[¶] Optimization of the complexes with NCO^- and NCS^- anions produced two modes of both HB and XB interactions (Figure S20 in the ESI. For clarity, the characteristics of the lower-energy XB and HB modes were used (involving S atom of NCS^- and N atom of NCO^-).

[$] If UV-Vis spectral changes related to the formation of HB complexes are explicitly taken into account, the expression for ΔAbs remains identical to that in eq 10, but with $\varepsilon = \Delta\varepsilon_{XB} + \Delta\varepsilon_{HB}K_{HB}/K_{XB}$, where $\Delta\varepsilon_{XB}$ and $\Delta\varepsilon_{HB}$ are the differences between extinction coefficients of the XB or HB complexes and the separate CHX_3 molecules (see p. S25 in the ESI). As such, inclusion of the spectral changes resulting from the formation of HB complexes does not change the values of the equilibria constants K_{HB} and K_{XB}. However, this analysis also shows that extinction coefficients ε resulting from the fittings may deviate more or less

significantly from the extinction coefficients of the XB complexes (the discussion of these values is beyond the scope of the current work).

†TD DFT computations indicated that excitation of an electron from the occupied MO residing on the anion to the LUMO residing on the CHX_3 moiety represent the main component of the most intense ground to exited state transitions in the XB complexes (i.e., they are charge transfer transitions). The main component of the most intense ground to exited state transitions in the HB complexes is related to the transition between MOs residing on the CHX_3 moiety (Figure S23 in the ESI).

[1] J. J. Colin, *Ann. Chim.* 1814, ***91***, 252–272.

[2] F. J. Guthrie, *Chem. Soc*. 1863, ***16***, 239–244**.**

[3] G. Cavallo, P. Metrangolo, R. Milani, T. Pilati, A. Priimagi, G. Resnati, G. Terraneo, *Chem. Rev.* 2016, ***116***, 2478–2601.

[4] L. C. Gilday, S. W. Robinson, T. A. Barendt, M. J. Langton, B. R. Mullaney, P. D. Beer, *Chem. Rev.* 2015, ***115***, 7118–7195.

[5] H. A. Benesi, J. H. Hildebrand, *J. Am. Chem. Soc.* **1949**, ***71***, 2703–2707.

[6] R. S. Mulliken, W. B. Person, *Molecular Complexes*. *A Lecture and Reprint Volume* Wiley: New York, **1969**.

[7] R. S. Mulliken, *J. Am. Chem. Soc.* 1952, ***74***, 811–824.

[8] H. A. Bent, *Chem. Rev.* 1968, ***68***, 587–648.

[9] R. A. Zingaro, R. M. Hedges, *J. Phys. Chem.* 1961, ***65***, 1132–1138.

[10] S. C. Blackstock, J. P. Lorand, J. K. Kochi, *J. Org. Chem.* 1987, ***52***, 1451–1460.

[11] R. D. Green, J. S. Martin, *J. Am. Chem. Soc.* 1968, ***90***, 3659–3668.

[12] J. F. Bertrán, M. Rodríguez, *Org. Magn. Resonance* 1979, ***12***, 92–94.

[13] P. Metrangolo, G. Resnati, *Chem. Eur. J.l* 2001, ***7***, 2511–2519.

[14] P. Metrangolo, P. Meyer, T. Pilati, G. Resnati, G. Terraneo, *Angew. Chem. Int. Ed.* 2008, ***47***, 6114–6127.

[15] A. Legon, *Angew. Chem. Int. Ed* 1999, ***38***, 2686–2714.

[16] P. Metrangolo, H. Neukirch, T. Pilati, G. Resnati, *Acc. Chem. Res.* 2005, ***38***, 386–395.

[17] P. Metrangolo, G. Resnati, *Science* 2008, ***321***, 918–919.

[18] P. Politzer, K. E. Riley, F. A. Bulat, J. S. Murray, *Comput. Theor. Chem.* 2012**,** ***998***, 2–8.

[19] T. Clark, *Faraday Discuss.* 2017, ***203***, 9–27.

[20] L. P. Wolters, F. M. Bickelhaupt, *ChemistryOpen* 2012, ***1***, 96–105.

[21] C. Wang, D. Danovich, Y. Mo, S. Shaik, *J. Chem. Theory Comput.* 2014, ***10*****,** 3726–3737.

[22] J. Thirman, E. Engelage, S. M. Huber, M. Head-Gordon, *Phys. Chem. Chem. Phys.* 2018, ***20*****,** 905–915.

[23] S. V. Rosokha, *Faraday Discuss.* 2017, ***203***, 315–332.

[24] S. J. Grabowski, *Chem. Rev.*, 2011, ***111*** , 2597–2625.

[25] E. Corradi, S. V. Meille, M. T. Messina, P. Metrangolo, G. Resnati, *Angew. Chem. Int. Ed* 2000, ***39*****,** 1782–1786.

[26] C. B. Aakeröy, M. Fasulo, N. Schultheiss, J. Desper, C. Moore, *J. Am. Chem. Soc.* 2007, ***129***, 13772–13773.

[27] I. Alkorta, F. Blanco, M. Solimannejad, J. Elguero, *J. Phys. Chem. A* 2008, ***112***, 10856–10863.

[28] P. M. J. Szell, J. Dragon, S. Zablotny, S. R. Harrigan, B. Gabidullin, D. L. Bryce, *New J. Chem.* 2018, ***42***, 10493-10501.

[29] A. Mukherjee, S. Tothadi, G. R. Desiraju, *Acc. Chem. Res.* 2014, ***47***, 2514–2524.

[30] K. Raatikainen, M. Cametti, K. Rissanen, *Beils. J. Org. Chem.* 2010, ***6***, 4.

[31] C. B. Aakeröy, S. Panikkattu, P. D. Chopade, J. Desper, *CrystEngComm* 2013, ***15***, 3125–3136.

[32] C. C. Robertson, R. N. Perutz, L. Brammer, C. A. Hunter, *Chem. Sci.* 2014, ***5***, 4179–4183.

[33] J. F. Bertrán, M. Rodríguez, *Revista de Ciencias Quimicas,* 1982, 1-8.

[34] L. Gilday, P.D. Beer, *Chem. Eur. J.* 2014, ***20***, 8379–8385.

[35] V. Stilinović, G. Horvat, T. Hrenar, V. Nemec, D. Cinčić, *Chem. Eur. J.* 2017, ***23***, 5175–5175.

[36] S. V. Rosokha, I. S. Neretin, T. Y. Rosokha, J. Hecht, J. K. Kochi, *Heteroatom Chem.* 2006, ***17***, 449–459.

[37] B. Koeppe, P. M. Tolstoy, H.-H. Limbach, *J. Am. Chem. Soc.* 2011, ***133***, 7897–7908.

[38] M. Cametti, K. Raatikainen, P. Metrangolo, T. Pilati, G. Terraneo, G. Resnati, *Org. Biomol. Chem.* 2012, ***10*****,** 1329–1333.

[39] N. Schulz, P. Sokkar,E. Engelage,S. Schindler, M. Erdelyi, E. Sanchez-Garcia, S. M. Huber, *Chem. Eur. J.* 2018, ***24***, 3464–3473.

[40] M. W. Hanna, A. L. Ashbaugh, *J. Phys. Chem.* 1964, ***68***, 811-816

[41] R. Foster, Organic Charge-Transfer Complexes, **2nd ed**; Academic Press Inc.: London, 1969; Ch. 7.

[42] P. Sabater, F. Zapata, A. Caballero, N. de la Visitación, I. Alkorta, J. Elguero, P. Molina, *J. Org. Chem.* 2016, ***81***, 7448–7458.

[43] S. Bhattacharya, S. K. Nayak, S. Chattopadhyay, M. Banerjee, A. Mukherjee, *J. Phys. Chem. A* 2001, ***105****,* 9865-9868

[44] S. Bhattacharya, S. K. Nayak, S. Chattopadhyay, M. Banerjee, A. Mukherjee, *J. Phys. Chem. B* 2003, ***107***, 11830-11834.

[45] S. Bhattacharya, M. Banerjee, A. K. Mukherjee, *Spectrochim. Acta Part A,* 2001, ***57***, 2409-2416.

[46] S. Bhattacharya, S. K. Nayak, S. Chattopadhyay, M. Banerjee, *Spectrochim. Acta Part A,* 2007, ***66*****,** 243-249.

[47] CSD version 5.39 (November 2017).

[48] X. Zhao, X. Pang, X. Yan, W. Jin, *Chinese J. Chem. Phys.* 2013, ***26***, 172–180.

[49]S. V. Rosokha, C. L. Stern,J. T. Ritzert, *Chem. Eur. J.* 2013, *19*, 8774–8788.

[50]S. V. Rosokha, C. L. Stern, A. Swartz, R. Stewart, *Phys. Chem. Chem. Phys.* 2014, ***16*****,** 12968–12979.

[51]S. V. Rosokha, A. Traversa, *Phys. Chem. Chem. Phys.* 2015, ***17***, 4989–4999.

[52] E. V. Anslyn, D. A. Dougherty, *Modern Physical Organic Chemistry*, University Science, Sausalito, CA, **2005,** p.186.

[53] Gaussian 09, Revision A.1, M. J. Frisch, G. W. Trucks, H. B. Schlegel, G. E. Scuseria, M. A. Robb, J. R. Cheeseman, G. Scalmani, V. Barone, B. Mennucci, G. A. Petersson, H. Nakatsuji, M. Caricato, X. Li, H. P. Hratchian, A. F. Izmaylov, J. Bloino, G. Zheng, J. L. Sonnenberg, M. Hada, M. Ehara, K. Toyota, R. Fukuda, J. Hasegawa, M. Ishida, T. Nakajima, Y. Honda, O. Kitao, H. Nakai, T. Vreven, J. A. Montgomery, Jr., J. E. Peralta, F. Ogliaro, M. Bearpark, J. J. Heyd, E. Brothers, K. N. Kudin, V. N. Staroverov, R. Kobayashi, J. Normand, K. Raghavachari, A. Rendell, J. C. Burant, S. S. Iyengar, J. Tomasi, M. Cossi, N. Rega, J. M. Millam, M. Klene, J. E. Knox, J. B. Cross, V. Bakken, C. Adamo, J. Jaramillo, R. Gomperts, R. E. Stratmann, O. Yazyev, A. J. Austin, R. Cammi, C. Pomelli, J. W. Ochterski, R. L. Martin, K. Morokuma, V. G. Zakrzewski, G. A. Voth, P. Salvador, J. J. Dannenberg, S. Dapprich, A. D. Daniels, O. Farkas, J. B. Foresman, J. V. Ortiz, J. Cioslowski, and D. J. Fox, Gaussian, Inc., Wallingford CT, **2009**.

[54] Y. Zhao and D. G. Truhlar, Theor. Chem. Acc., 2008, **120**, 215–241.

[55] J.Tomasi, B. Mennucci, R. Cammi, *Chem. Rev.* 2005, **105**, 2999−3093.

[56] D. M. Ivanov, A. S. Novikov, I. V. Ananyev, Y. V. Kirina, V. Yu. Kukushkin, *Chem. Comm.* 2016, **52**, 5565–5568.

[57] D. M. Ivanov, M. A. Kinzhalov, A. S. Novikov, I. V. Ananyev, A. A. Romanova, V. P. Boyarskiy, M. Haukka, V. Y. Kukushkin, *Cryst. Growth Des.* 2017, ***17***, 1353–1362.

[58] H. G. Loehr, A. Engel, H. P. Josel, F. Voegtle, W. Schuh, H. Puff, *J. Org. Chem.* 1984, ***49***, 1621–1627.

[59] W.-W. du Mont, V. Stenzel, J. Jeske, P. G. Jones, A. Sebald, S. Pohl, W. Saak, M. Baetcher, *Inorg. Chem.* 1994, ***33***, 1502–1505.

]60] H. Bock, S. Holl, *Z. Naturforsch. B* 2014, **56**, 152–163.

[61] S. V. Rosokha, M. K. Vinakos, *Cryst. Growth Des.* 2012, ***12***, 4149–4156.

[62] T. V. Serebryanskaya, A. S. Novikov, P. V. Gushchin, M. Haukka, R. E. Asfin, P. M. Tolstoy, V. Y. Kukushkin, *Phys. Chem. Chem. Phys.* 2016, ***18*****,** 14104–14112.